Bioorganic & Medicinal Chemistry Letters 22 (2012) 2444–2449

Contents lists available at SciVerse ScienceDirect

Bioorganic & Medicinal Chemistry Letters

journal homepage: www.elsevier.com/locate/bmcl

Structure based design of iminohydantoin BACE1 inhibitors: Identification of an orally available, centrally active BACE1 inhibitor

Jared N. Cumming *,†, Elizabeth M. Smith, Lingyan Wang, Jeffrey Misiaszek, James Durkin, Jianping Pan, Ulrich Iserloh, Yusheng Wu, Zhaoning Zhu, Corey Strickland, Johannes Voigt, Xia Chen, Matthew E. Kennedy, Reshma Kuvelkar, Lynn A. Hyde, Kathleen Cox, Leonard Favreau, Michael F. Czarniecki, William J. Greenlee, Brian A. McKittrick, Eric M. Parker, Andrew W. Stamford *,‡

Merck Research Laboratories, 2000 Galloping Hill Road, Kenilworth, NJ 07033, USA

ARTICLE INFO

Article history:
Received 11 January 2012
Revised 3 February 2012
Accepted 6 February 2012
Available online 16 February 2012

Keywords:
BACE
β-Secretase
Alzheimer's disease
Iminohydantoin
In vivo

ABSTRACT

From an initial lead **1**, a structure-based design approach led to identification of a novel, high-affinity iminohydantoin BACE1 inhibitor that lowers CNS-derived Aβ following oral administration to rats. Herein we report SAR development in the S3 and F′ subsites of BACE1 for this series, the synthetic approaches employed in this effort, and in vivo data for the optimized compound.

Alzheimer's disease (AD) is a chronic, progressive, ultimately fatal neurodegenerative disease that occurs predominantly in the elderly population. Current treatments, which consist of the acetylcholineesterase inhibitors and the NMDA receptor antagonist memantine, temporarily slow the cognitive decline that is associated with the disease, but do not alter the underlying neurodegenerative process and therefore have no effect on disease progression.[1] Given the devastating effects of AD on patients and their families as well the increasing societal burden as a result of aging populations worldwide, disease-modifying treatments are urgently needed.[2,3]

The characteristic neuropathological hallmarks of AD are the presence of extracellular amyloid plaques comprised predominantly of the amyloid peptide Aβ42 and intracellular tangles of hyperphosphorylated protein tau in the cortex and hippocampus. According to the amyloid hypothesis, accumulation of Aβ, most likely as soluble oligomeric and protofibrillar forms, is causative of the disease.[4,5] The amyloid peptides Aβ40 and Aβ42 are formed by sequential cleavage of the amyloid precursor protein (APP), first by the aspartyl protease β-APP cleaving enzyme 1 (BACE1)[6–10] which yields the soluble APP N-terminal fragment sAPPβ and the membrane bound C-terminal fragment C100. C100 is subsequently cleaved by γ-secretase to yield the plaque-forming Aβ40 and Aβ42 peptides. Inhibition of BACE1 is highly attractive as a potential disease-modifying approach for AD. BACE1 knockout mice are viable with no overt abnormalities, do not synthesize Aβ and display only a moderate peripheral nerve hypomyelination phenotype that is due to the loss of BACE1-mediated processing of Type III Neuregulin.[11–15] Furthermore, BACE1 is a well-characterized aspartyl protease, and is amenable to structure-based drug design.[16] However, the identification of small molecule BACE inhibitors that penetrate the CNS and lower CNS-derived Aβ has proved to be exceptionally challenging. This communication describes the evolution of novel iminohydantoin BACE1 inhibitors resulting in the identification of a potent inhibitor that lowers cerebrospinal fluid (CSF) Aβ in rats following oral administration.

We have previously described the design of a cyclic acylguanidine series of BACE1 inhibitors exemplified by the diphenyl iminohydantoin **1**, an inhibitor of BACE1 with low micromolar affinity (Fig. 1).[17,18] Based on its high ligand efficiency (LE), inherent selectivity over the related aspartyl protease cathepsin D, and favorable pharmacokinetic properties, **1** was considered to be an ideal lead for further optimization. An X-ray crystal structure of

* Corresponding authors. Tel.: +1 732 594 3049 (J.N.C.), tel.: +1 732 594 1960 (A.W.S.).
E-mail addresses: jared.cumming@merck.com (J.N. Cumming), andrew.stamford@merck.com (A.W. Stamford).
† Present address: Merck Research Laboratories, 126 E. Lincoln Ave., RY121-274, Rahway, NJ 07065, USA
‡ Present address: Merck Research Laboratories, 126 E. Lincoln Ave., PO Box 2000, Rahway, NJ 07065, USA

0960-894X/$ - see front matter © 2012 Elsevier Ltd. All rights reserved.
doi:10.1016/j.bmcl.2012.02.013

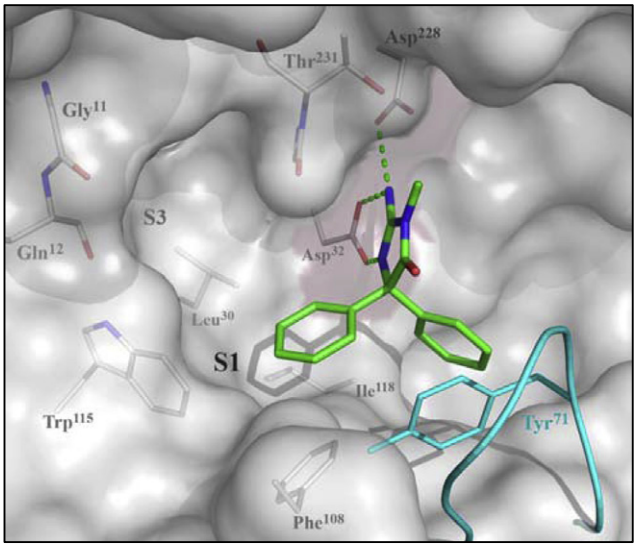

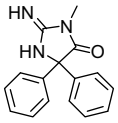

Compound **1**
MW: 265, cLogP: 1.9
ligand efficiency: 0.37
BACE1 K_i: 3.6 μM
cell Aβ40 IC_{50}: 12 μM
rat $AUC_{0\text{-}6h}$ 10 mg/kg p.o.: 5 μM·h
b/p ratio: 1.8
Cath-D: 38% inhib. @ 50 μM

Figure 1. Profile and binding mode of iminohydantoin lead **1**.

1 complexed to BACE1 revealed the following characteristics (Fig. 1). The amidine motif of the iminohydantoin core participates in an H-bond donor–acceptor complex with two Asp residues, Asp^{32} and Asp^{228}, at the active site of BACE1. The S1 pocket of BACE1, defined by several hydrophobic residues including Leu^{30}, Phe^{108}, Trp^{115} and Ile^{118}, is occupied by one of the phenyl groups of **1**. The other phenyl group of **1** occupies space near S2′ that we have termed F′. In the X-ray crystal structure of the peptidomimetic inhibitor OM99-2 and BACE1, this region is occupied by Tyr^{71} of the flap loop in its closed conformation.[19] In the X-ray crystal structure of **1**,[20] the flap loop is fairly well-ordered but more open in comparison with the closed, substrate-bound form, with the aromatic ring of Tyr^{71} engaged in a hydrophobic interaction with the inhibitor. In this communication we report the optimization of lead iminohydantoin **1** enabled by structure-based design to afford a novel, high-affinity BACE1 inhibitor that lowers CNS-derived Aβ following oral administration to rats.

An attractive approach to gain affinity while maintaining the high LE of **1** was to occupy the adjacent S3 pocket by substitution on the phenyl group residing in S1. In silico docking experiments indicated that 3-biaryl substitution offered the possibility of occupying the contiguous S1–S3 pockets.[21] To this end a series of biaryl derivatives was prepared and evaluated as BACE1 inhibitors. The synthesis of the biaryl derivatives is shown in Scheme 1.

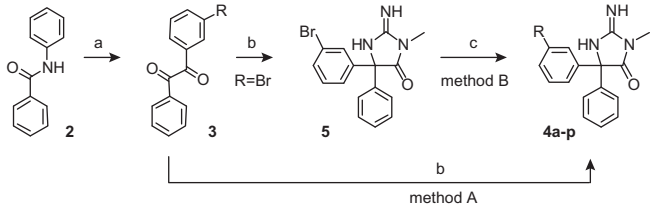

Scheme 1. Reagents and conditions: (a) (i) $SOCl_2$, toluene, reflux, (ii) aldehyde, 1,3-dimethyl-imidazolium iodide, NaH, THF, (iii) 1 N HCl, THF; (b) *N*-methylguanidine hydrochloride, Et_3N, EtOH, reflux; (c) $RB(OH)_2$, $Pd(dppf)Cl_2$, K_2CO_3, toluene, H_2O, microwave, 150 °C.

N-phenyl-benzamide **2** was converted into the chloroimidate which was then reacted with the appropriate benzaldehyde and 1,3-dimethylimidazolium iodide to afford the benzil derivative **3**.[22] Condensation of **3** with methylguanidine hydrochloride afforded the desired targets **4**. Alternatively, the benzil route was used to prepare the bromophenyl iminohydantion **5**. Suzuki coupling of **5** with the appropriate boronic acid gave the desired products **4**.

Gratifyingly, several 3-biaryl modifications resulted in inhibitors with improved BACE1 affinity (Table 1). Thus, derivatization of the S1 phenyl group as an appropriately (3′-substituted) biphenyl-3-yl resulted in an order of magnitude improvement in affinity with analogs **4b**, **4d**–**4h** displaying sub-micromolar K_i values. The importance of the 3′-substituent is highlighted by comparison to the parent biphenyl analog **4a** whereby incorporation of an unsubstituted phenyl group resulted in essentially no improvement of affinity.

BACE1 X-ray crystal structures obtained with the racemic 3-methoxyphenyl and pyridin-3-yl analogs **4b** and **4j** revealed density only for the (*R*) enantiomers, confirming the predicted binding modes with the biaryl motif occupying the S1 and S3 pockets.[24] For the pyridin-3-yl analog, the pyridine nitrogen is presumed to face the entrance of the S3 sub-pocket which was inferred by the observation of a crystallographic water molecule at a distance of 2.9 Å from the pyridine nitrogen (Fig. 2). In the case of the

Table 1
BACE1 affinities of iminohydantoins **4a**–**p**[23]

Compd	R	BACE1 K_i (μM)	Method (Scheme 1)
4a	Ph	3.3	B
4b	3-MeOPh	0.19	B
4c	4-MeOPh	3.8	B
4d	3-EtOPh	0.46	B
4e	3-F	0.72	A
4f	3-Cl	0.30	A
4g	3-Me	0.55	A
4h	3-CN	0.37	A
4i	Pyridin-2-yl	1.9	B
4j	Pyridin-3-yl	0.53	B
4k	Pyridin-4-yl	3.8	B
4l	Pyrazin-5-yl	0.31	B
4m	5-Methylpyridin-3-yl	0.43	B
4n	5-Cyanopyridin-3-yl	0.47	B
4o	5-Fluoropyridin-3-yl	0.29	B
4p	5-Chloropyridin-3-yl	0.09	B

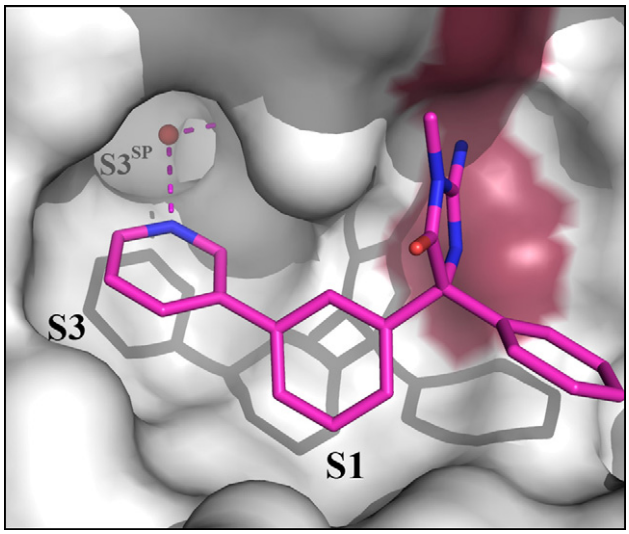

Figure 2. X-ray crystal structure of **4j** bound to BACE1.

Table 2
BACE1 K_i, cell IC_{50} and selectivity of **6a–b** and **7a–b**[23]

Compd	R	BACE1 K_i (μM)	Cell Aβ40 IC_{50} (μM)	Fold selectivity: BACE1 versus Cathepsin D
6a	(*R*)-3-MeOPh	0.08	2.3	120
6b	(*S*)-3-MeOPh	6.0	nd[a]	19
7a	(*R*)-Pyridin-3-yl	0.11	0.63	455
7b	(*S*)-Pyridin-3-yl	1.7	nd[a]	6

[a] Not determined.

3-methoxyphenyl analog **4c**, the methoxy group projects into the S3 subpocket displacing the aforementioned water molecule (Fig. 2). The enantiomers of both the 3-methoxyphenyl (**6a**, **6b**) and pyridin-3-yl analogs (**7a**, **7b**) were prepared (Table 2)[25] and in each case the (*R*) absolute configuration was assigned to the more active enantiomer of each pair. Compounds **6a** and **7a** possess LE values of 0.35 and 0.36 respectively, which compare favorably to that of **1**. These compounds were also active in a cellular assay of BACE1-mediated processing of APP, with the less lipophilic pyridyl analog **7a** showing a smaller shift between the K_i and cell Aβ40 IC_{50} in comparison to the corresponding methoxyphenyl analog **6a**.

Our attention next turned toward examining the effect of modifications of the phenyl group that resides in F′ with respect to BACE1 affinity and cell activity, fixing the biaryl motif as a 3′-chloro-3-biphenyl moiety. Synthesis of these F′ modified analogs is described in Scheme 2. The appropriate ketone starting material **8** was converted to the corresponding hydantoin **9** via Bucherer–Berg conditions. Exploiting the relative acidity of the *N*3 proton, the hydantoin was smoothly methylated at *N*3 using dimethylformamide-dimethylacetal (DMF-DMA) in essentially quantitative yield to give **10**. Conversion of the more reactive C2 carbonyl to the corresponding thiocarbonyl **11** with Lawesson's reagent followed by oxidative amination gave the iminohydantoin **12**. Suzuki coupling of **12** was conducted using polystyrene-immobilized triphenylphosphine–palladium complex to install the 3′-chlorophenyl moiety directly without protection of the acyl guanidine moiety yielding the desired products **13**. The yields for this sequence were generally good to excellent.

As noted in Table 3, the majority of analogs in which the phenyl was replaced by an alkyl (**13a–c**) or cycloalkyl group (**13f–g**) had affinities similar to that of the phenyl analog **4f**. Notably, the cyclopropyl analog **13d** was about sixfold more potent than **4f** (47 nM vs 300 nM). Heterocyclic replacements resulted in analogs of similar to somewhat reduced affinities (**13j–k**, **13m–o**) with the exception of the pyridine-4-yl analog **13l** which was essentially inactive. Cellular activity was generally in the micromolar range, with potency shifts relative to K_i values ranging from about sevenfold (**13a** and **13j**) up to 40-fold (**13d**).

Having identified cyclopropyl as a substituent that confers higher affinity than phenyl, further modifications to the biaryl motif were conducted with an objective of improving BACE1 affinity and reducing the shift between the BACE1 K_i and cell IC_{50}. To this end a strategy of modifying the distal phenyl group was implemented, with an emphasis on reduction of cLog*P* by replacing chloro with more polar substituents and the distal phenyl group with a pyridin-3-yl group. Synthesis and derivatization of the required cyclopropyl iminohydantoin core to enable this approach is described in Scheme 3. Copper-mediated addition of cyclopropylmagnesium chloride to 3-bromobenzoyl chloride **14** gave cyclopropyl ketone **15** that was converted to the iminohydantoin **16** in four steps and 50% overall yield following procedures analogous to those in Scheme 2. Suzuki coupling of **16** to form biaryl derivatives **17** proceeded directly without the need for protection of the iminohydantoin. Complementarily, the bromophenyl intermediate **16** was also converted to its boronate ester **18**, which underwent Suzuki coupling with aryl bromides to give desired biaryl derivatives.

Table 3
BACE1 affinity and cell activity of **13a–o**[23]

Compd	R′	BACE1 K_i (nM)	Aβ40 IC_{50} (nM) (fold shift relative to K_i)	cLog*P*
13a	Me	720	4,800 (7×)	3.4
13b	Et	450	5,300 (12×)	3.9
13c	*i*-Pr	320	4,600 (15×)	4.3
13d	*c*-Pr	47	1,900 (40×)	3.8
13e	*c*-Bu	110	2,800 (25×)	4.3
13f	*c*-Pn	470	6,900 (15×)	4.9
13g	*c*-He×	470	11,000 (23×)	5.4
13h	1-Methyl-*c*-Pr	190	6,000 (31×)	4.3
13i	*c*-Pr-methyl	350	9,500 (27×)	4.4
13j	Pyridin-2-yl	860	5,900 (7×)	3.0
13k	Pyridin-3-yl	170	4,400 (26×)	3.0
13l	Pyridin-4-yl	>10,000	nd[a]	3.0
13m	Pyrmidin-5-yl	830	21,000 (25×)	2.0
13n	Pyrmidin-2-yl	1200	>10,000	2.0
13o	Thiazol-2-yl	1200	>10,000	2.8

[a] Not determined.

Inspection of the data in Table 4 reveals that reduction of the cLog*P* value below 3 results in significantly reduced cellular potency shifts (**17c–i**). In addition, where tested, the compounds were of equal or higher affinity against BACE2, a peripherally localized enzyme with significant homology to BACE1.[26] While a

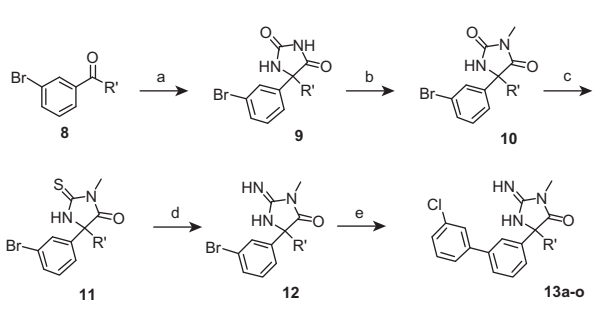

Scheme 2. Reagents and conditions. (a) $(NH_4)_2CO_3$, KCN, 120 °C; (b) DMF-DMA, 100 °C; (c) Lawesson's reagent, 100 °C; (d) *t*-BuOOH, NH_4OH; (e) 3-ClPhB$(OH)_2$, PS-Ph_3P-Pd, K_2CO_3, *i*-PrOH, microwave, 110 °C.

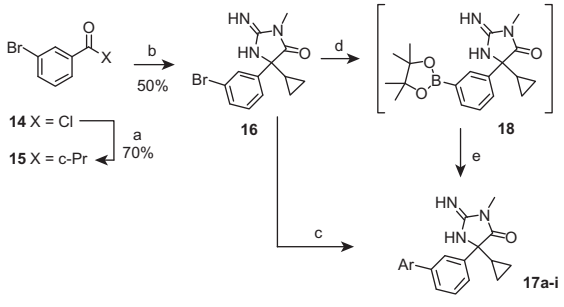

Scheme 3. Reagents and conditions. (a) *c*-PrMgCl, CuCl, LiCl, −60 °C; (b) Steps a–d, Scheme 2; (c) ArB$(OH)_2$, PS-Ph_3P-Pd, K_2CO_3, *i*-PrOH, microwave, 110 °C; (d) Bis(pinacolato)diboron, $PdCl_2$dppf, KOAc, DMSO, 120 °C; (e) ArBr, PS-Ph_3P-Pd, K_2CO_3, DMSO, 120 °C.

Table 4
BACE1 affinity and cell Aβ40 activity of **17a–i**[23]

Compd	Ar	BACE1 K_i (nM)	Aβ40 IC_{50} (nM) (fold shift relative to K_i)	cLog*P*	BACE2 K_i (nM)
17a	3,5-Cl_2Ph	30	2400 (80×)	4.5	nd[a]
17b	3-MeOPh	99	1600 (16×)	3.0	7.8
17c	3-CNPh	130	940 (7×)	2.5	30
17d	Pyridin-3-yl	270	880 (3×)	1.6	360
17e	5-MeO-Pyridin-3-yl	100	390 (4×)	2.0	11
17f	5-CN-Pyridin-3-yl	270	610 (2×)	1.2	170
17g	5-F-Pyridin-3-yl	160	800 (5×)	1.8	139
17h	5-Cl-Pyridin-3-yl	59	380 (6×)	2.4	nd[a]
17i	5-Me-Pyridin-3-yl	250	640 (3×)	2.1	68

[a] Not determined.

number of groups have reported inhibitors with selectivity for BACE1 over BACE2,[27,28] the lack of any overt phenotype reported for BACE2 knockout mice suggests that no liabilities are expected to arise from BACE2 inhibition,[29] and indeed recent reports suggest there may be a benefit in glucose homeostasis.[30]

The chloropyridine analog **17h** was among the most potent compounds with respect to both K_i and cellular activity, and an X-ray crystal structure of this compound with BACE1 was obtained (Fig. 3).[31] As was observed for **4b** and **4j**, only density for the 5-(*R*) enantiomer was observed and the binding features of this analog were highly conserved in comparison with the earlier compounds. The cyclopropyl substituent resides in the F′ pocket and is engaged in a hydrophobic interaction with Tyr[71] of the well-ordered flap. The chloropyridyl substituent resides in the S3 sub-pocket with the chloro substituent positioned at the entrance of the S3 sub-pocket.

The (*R*) enantiomer of the chloropyridine analog, **19** was prepared and subjected to more detailed characterization. Synthesis of **19** was achieved by hydrolysis of the racemic hydantoin intermediate **20** to give amino acid **21** (Scheme 4). Conversion of **21** to its methyl ester followed by chiral HPLC gave the (*R*)-enantiomer **22**. Treatment of **22** with thiophosgene afforded the thioisocyanate which upon reaction with methylamine cyclized to the thiohydantoin **23**. Elaboration of **23** to chloropyridine **19** was achieved following procedures analogous to those outlined in Scheme 2.

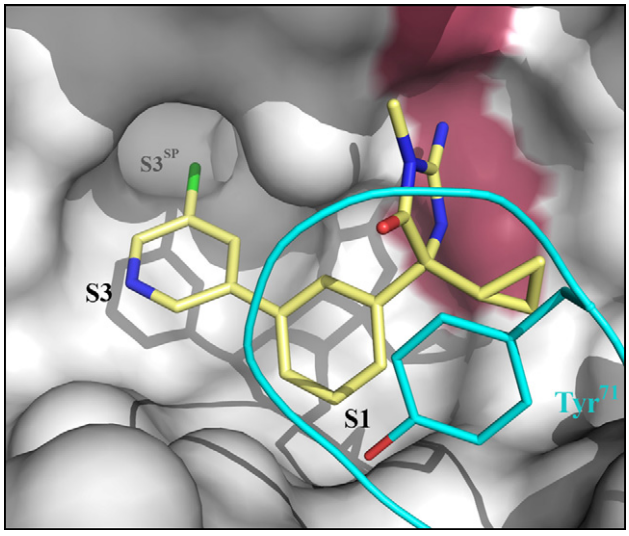

Figure 3. X-ray crystal structure of **17h** bound to BACE1.

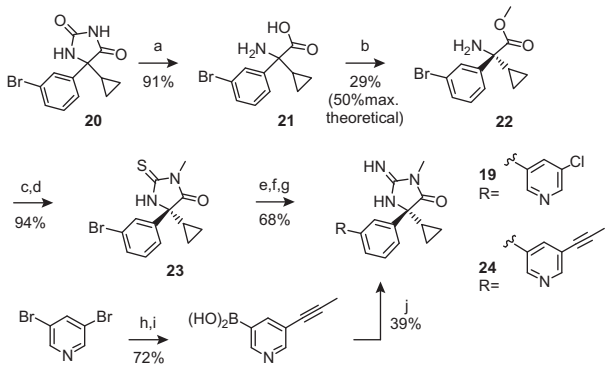

Scheme 4. Reagents and conditions. (a) 1 N aq. KOH, 185 °C, 24 h; (b) (i) $TMSCHN_2$, (ii) Chiralpak AS column (Diacel, 5 × 50 cm, 20 mm), 0.5% *i*-PrOH/hexanes, 65 mL/min), second eluting isomer; (c) $Cl_2C(S)$, DCM, sat. aq. $NaHCO_3$; (d) $MeNH_2$–HCl, DIEA, 70 °C; (e) *t*-BuOOH, NH_4OH; (f) bis-(pinacolato)diboron, $PdCl_2$dppf, KOAc, DMSO, 120 °C; (g) 3,5-dichloropyridine, PS-Ph_3P-Pd, aq. K_2CO_3, DMSO, 120 °C; (h) 1-(trimethylsilyl)propyne, $Pd(PPh_3)_4$, CuI, Et_3N, *n*-Bu_4NF, PhMe, rt; (i) BuLi, B(O*i*-Pr)$_3$, THF/PhMe, −40 to −10 °C then aq. NH_4OH; (j) Product of step (e), $PdCl_2(dppf)CH_2Cl_2$, aq. K_2CO_3, dioxane, 65 °C.

Compound **19** binds to BACE1 with good affinity, very high LE (0.44) and is about 350-fold selective for BACE1 versus cathepsin D (Table 5). In a rat oral pharmacokinetic screen, the compound achieved good plasma exposure.[32] Subsequent efforts focused on further improving BACE1 affinity explored replacement of the chloro by a propynyl group, which based on its linear trajectory afforded the possibility of binding more deeply in the S3 sub-pocket. The resultant analog **24** (K_i 5.4 nM, Table 5), synthesized as outlined in Scheme 4, was about a fivefold more potent inhibitor of BACE1 compared to the chloro analog **19**. Cellular activity of **24** was also improved relative to **19**, with **24** displaying a cell IC_{50} of 82 nM. Replacement of the chloro substituent by propynyl is also beneficial for BACE1 selectivity versus cathepsin D, with selectivity of **24** increasing to 7,500-fold. An X-ray crystal structure of **24** and BACE1 was highly consistent with that observed for chloro analog,[23] with the major difference being protrusion of the propynyl methyl group deep into the S3 sub-pocket where it is likely engaged in a favorable hydrophobic interaction with Ala[396] (Fig. 4).[33] In a rat pharmacokinetic screen **24** showed excellent plasma exposure following oral administration.[32]

Based on its favorable overall profile, the ability of compound **24** to lower Aβ40 levels in rat plasma and CSF was evaluated (Fig. 5). A single oral dose of 30 mg/kg elicited a 54% reduction of CSF Aβ40 three hours post dose relative to vehicle-treated control, indicating inhibition of BACE1 localized in the CNS. In the same experiment, plasma Aβ40 was reduced by 85%. The plasma exposure of **24** at that dose was 4.2 μM with a brain/plasma ratio of 0.2, a value that was in good agreement with the rat oral pharmacokinetic screen.

In summary, optimization of the iminohydantoin class of BACE1 inhibitors has afforded **24** as a potent, selective, brain penetrant

Table 5
Profiles of **19** and **24**[23]

Compd	BACE1 K_i (nM)	Cell Aβ40 IC_{50} (nM)	Fold selectivity: BACE1 versus Cathepsin D	Rat $AUC_{0\text{-}6h}$ (μM h)[a]	Brain/plasma	cLog*P*
19	21	150	350	3.1	nd[b]	2.4
24	5.4	82	7,500	17.9	0.3	2.4

[a] 10 mg/kg orally administered as a hydroxypropyl-β-cyclodextrin solution in 20%.
[b] Not determined.

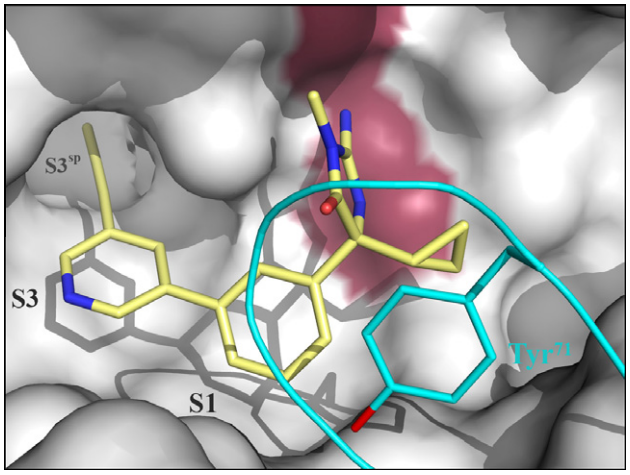

Figure 4. X-ray crystal structure of **24** bound to BACE1.

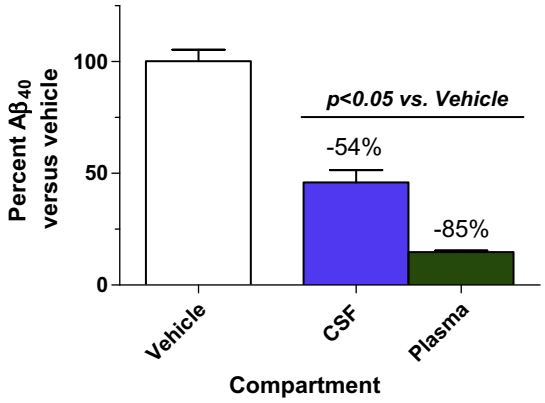

Figure 5. Inhibition of CSF and plasma Aβ40 in Sprague–Dawley rats 3 h after a single oral 30 mg/kg dose of **24**.

and orally active BACE1 inhibitor, demonstrating that inhibitors from this class hold promise as potential disease-modifying agents for AD. Subsequent reports will detail further optimization efforts that resulted in inhibitors with improved cell and in vivo potency.

Acknowledgements

Use of the IMCA-CAT beamline at the Advanced Photon Source was supported by the companies of the Industrial Macromolecular Crystallography Association through a contract with Hauptman-Woodward Medical Research Institute. Use of the Advanced Photon Source was supported by the U.S. Department of Energy, Office of Science, Office of Basic Energy Sciences, under Contract No. DE-AC02-06CH11357.

References and notes

1. Blennow, K. M.; de Leon, J.; Zetterberg, H. *Lancet* **2006**, *368*, 387.
2. Ferri, C. P.; Prince, M.; Brayne, C.; Brodaty, H.; Fratiglioni, L.; Ganguli, M.; Hall, K.; Hasegawa, K.; Hendrie, H.; Huang, Y.; Jorm, A.; Mathers, C.; Menezes, P. R.; Rimmer, E.; Marcia Scazufca, M. *Lancet* **2005**, *366*, 2112.
3. Alzheimer's Association. 2011 Alzheimer's Disease Facts and Figures. Alzheimer's & Dementia: J. Alzheimer's Assoc. **2011**, *7*, 208.
4. (a) Wolfe, M. S. In *Emerging Drugs and Targets for Alzheimer's Disease: Volume 1: Beta-Amyloid*; Martinez, A., Ed.; Tau Protein and Glucose Metabolism; Royal Society of Chemistry: Cambridge, 2010; Vol. 1, pp 3–18; (b) Klyubin, I.; Betts, V.; Welzel, A. T.; Blennow, K.; Zetterberg, H.; Wallin, A.; Lemere, C. A.; Cullen, W. K.; Peng, Y.; Wisniewski, T.; Selkoe, D. J.; Anwyl, R.; Walsh, D. M.; Rowan, M. J. *J. Neurosci.* **2008**, *28*, 4231; (c) Hock, C.; Konietzko, U.; Streffer, J. R.; Tracy, J.; Signorell, A.; Muller-Tillmanns, B.; Lemke, U.; Henke, K.; Moritz, E.; Garcia, E.; Wollmer, M. A.; Umbricht, D.; de Quervain, D. J.; Hofmann, M.; Maddalena, A.; Papassotiropoulos, A.; Nitsch, R. M. *Neuron* **2003**, *38*, 547; (d) Younkin, S. G. *Ann. Neurol.* **1995**, *37*, 287.
5. (a) Hardy, J.; Selkoe, D. J. *Science* **2002**, *297*, 353; (b) Selkoe, D. J. *Phys. Rev.* **2001**, *81*, 741.
6. (a) Vassar, R.; Bennett, B. D.; Babu-Khan, S.; Kahn, S.; Mendiaz, E. A.; Denis, P.; Teplow, D. B.; Ross, S.; Amarante, P.; Loeloff, R.; Luo, Y.; Fisher, S.; Fuller, J.; Edenson, S.; Lile, J.; Jarosinski, M. A.; Biere, A. L.; Curran, E.; Burgess, T.; Louis, J. C.; Collins, F.; Treanor, J.; Rogers, G.; Citron, M. *Science* **1999**, *286*, 735; as well as a comprehensive review: (b) Vassar, R.; Kandalepas, P. C. *Alzheimers Res. Ther.* **2011**, *3*, 20.
7. Sinha, S.; Anderson, J. P.; Barbour, R.; Basi, G. S.; Caccavello, R.; Davis, D.; Doan, M.; Dovey, H. F.; Frigon, N.; Hong, J.; Jacobson-Croak, K.; Jewett, N.; Keim, P.; Knops, J.; Lieberburg, I.; Power, M.; Tan, H.; Tatsuno, G.; Tung, J.; Schenk, D.; Seubert, P.; Suomensaari, S. M.; Wang, S.; Walker, D.; Zhao, J.; McConlogue, L.; John, V. *Nature* **1999**, *402*, 537.
8. Yan, R.; Bienkowski, M. J.; Shuck, M. E.; Miao, H.; Tory, M. C.; Pauley, A. M.; Brashier, J. R.; Stratman, N. C.; Mathews, W. R.; Buhl, A. E.; Carter, D. B.; Tomasselli, A. G.; Parodi, L. A.; Heinrikson, R. L.; Gurney, M. E. *Nature* **1999**, *402*, 533.
9. Hussain, I.; Powell, D.; Howlett, D. R.; Tew, D. G.; Meek, T. D.; Chapman, C.; Gloger, I. S.; Murphy, K. E.; Southan, C. D.; Ryan, D. M.; Smith, T. S.; Simmons, D. L.; Walsh, F. S.; Dingwall, C.; Christie, G. *Mol. Cell Neurosci.* **1999**, *14*, 419.
10. Lin, X.; Koelsch, G.; Wu, S.; Downs, D.; Dashti, A.; Tang, J. *Proc. Natl. Acad. Sci. U.S.A.* **2000**, *97*, 1456.
11. Cai, H.; Wang, Y.; McCarthy, D.; Wen, H.; Borchelt, D. R.; Price, D. L.; Wong, P. C. *Nat. Neurosci.* **2001**, *4*, 233.
12. Luo, Y.; Bolon, B.; Kahn, S.; Bennett, B. D.; Babu-Khan, S.; Denis, P.; Fan, W.; Kha, H.; Zhang, J.; Gong, Y.; Martin, L.; Louis, J. C.; Yan, Q.; Richards, W. G.; Citron, M.; Vassar, R. *Nat. Neurosci.* **2001**, *4*, 231.
13. Roberds, S. L.; Anderson, J.; Basi, G.; Bienkowski, M. J.; Branstetter, D. G.; Chen, K. S.; Freedman, S. B.; Frigon, N. L.; Games, D.; Hu, K.; Johnson-Wood, K.; Kappenman, K. E.; Kawabe, T. T.; Kola, I.; Kuehn, R.; Lee, M.; Liu, W.; Motter, R.; Nichols, N. F.; Power, M.; Robertson, D. W.; Schenk, D.; Schoor, M.; Shopp, G. M.; Shuck, M. E.; Sinha, S.; Svensson, K. A.; Tatsuno, G.; Tintrup, H.; Wijsman, J.; Wright, S.; McConlogue, L. *Hum. Mol. Genet.* **2001**, *10*, 1317.
14. Willem, M.; Garratt, A. N.; Novak, B.; Citron, M.; Kaufmann, S.; Rittger, A.; DeStrooper, B.; Saftig, P.; Birchmeier, C.; Haass, C. *Science* **2006**, *314*, 664.
15. Hu, X.; Hicks, C. W.; He, W.; Wong, P.; Macklin, W. B.; Trapp, B. D.; Yan, R. *Nat. Neurosci.* **2006**, *9*, 1520.
16. Vajdos, F. C.; Shanmugasundaram, V.; Tomasselli, A. G. In *BACE Lead Target for Orchestrated Therapy in Alzheimer's Disease*; John, Varghese, Ed.; John Wiley and Sons, 2010.
17. (a) Zhu, Z.; Sun, Z.-Y.; Ye, Y.; Voigt, J.; Strickland, C.; Smith, E. M.; Cumming, J.; Wang, L.; Wong, J.; Wang, Y.-S.; Wyss, D. F.; Chen, X.; Kuvelkar, R.; Kennedy, M. E.; Favreau, L.; Parker, E.; McKittrick, B. A.; Stamford, A.; Czarniecki, M.; Greenlee, W.; Hunter, J. C. *J. Med. Chem.* **2010**, *53*, 951. Other researchers independently identified the same diphenyliminohydantoin structure, c.f.; (b) Malamas, M. S.; Robichaud, A.; Erdei, J.; Quagliato, D.; Solvibile, W.; Zhou, P.; Morris, K.; Turner, J.; Wagner, E.; Fan, K.; Olland, A.; Jacobsen, S.; Reinhart, P.; Riddell, D.; Pangalos, M. *Bioorg. Med. Chem. Lett.* **2010**, *20*, 6597.
18. Wang, Y.-S.; Strickland, C.; Voigt, J. H.; Kennedy, M. E.; Beyer, B. M.; Senior, M. M.; Smith, E. M.; Nechuta, T. L.; Madison, V. S.; Czarniecki, M.; McKittrick, B. A.; Stamford, A. W.; Parker, E. M.; Hunter, J. C.; Greenlee, W. J.; Wyss, D. F. *J. Med. Chem.* **2010**, *53*, 942.
19. Hong, L.; Koelsch, G.; Lin, X.; Wu, S.; Terzyan, S.; Ghosh, A. K.; Zhang, X. C.; Tang, J. *Science* **2000**, *290*, 150.
20. Coordinates for the X-ray structure of compound **1** complexed with BACE1 have been deposited in the Protein Data Bank (www.rcsb.org), and can be accessed under PDB ID 4DJU.
21. Jaguar, version 5.5; Schrödinger LLC: New York.
22. Miyashita, A.; Matsuda, H.; Higashino, T. *Chem. Pharm. Bull.* **1992**, *40*, 2627.
23. Inhibitor Ki values at purified human BACE1, BACE2, and Cathepsin D (Cath-D) were determined using a FRET-peptide substrate hydrolysis assay. Cellular IC50 values for reduction of Aβ40 production were determined in stably transfected HEK293-APPswe/lon cells. The protocols for these assays have been previously described in reference 17 (Zhu, et al.). All values reported are the average of a minimum of two independent determinations.
24. Coordinates for the X-ray structures of compounds **4b** and **4j** complexed with BACE1 have been deposited in the Protein Data Bank (www.rcsb.org), and can be accessed under PDB IDs 4DJV and 4DJW, respectively.
25. Separation of **4b** on a Chirocel Preparative OJ column eluted with isopropanol (0.1% triethylamine): hexane (0.1% triethylamine) in a ratio of 1:3 gave **6a** (t_R 23.3 min) as the later eluting component. Separation of the 3-bromophenyl intermediate **5** on a Chirocel Preparative OJ column eluted with isopropanol (0.1% triethylamine): hexane (0.1% triethylamine) in a ratio of 3: 17 gave the (*R*)-enantiomer of **5** (t_R 38. 6 min.) as the later eluting component, which was converted to **7a** via Suzuki coupling with pyridin-3-ylboronic acid.
26. De Strooper, B.; Vasar, R.; Golde, T. *Nat. Rev. Neurol.* **2010**, *6*, 99.
27. Malamas, M. S.; Erdei, J.; Gunawan, I.; Barnes, K.; Hui, Y.; Johnson, M.; Robichaud, A.; Zhou, P.; Yan, Y.; Solvibile, W.; Turner, J.; Fan, K. Y.; Chopra, R.; Bard, J.; Pangalos, M. N. *Bioorg. Med. Chem. Lett.* **2011**, *21*, 5164.
28. Al-Tel, T. H.; Semreen, M. H.; Al-Qawasmeh, RA.; Schmidt, M. F.; El-Awadi, R.; Ardah, M.; Zaarour, R.; Rao, S. N.; El-Agnaf, O. *J. Med. Chem.* **2011**, *54*, 8373.

29. Dominguez, D.; Tournoy, J.; Hartmann, D.; Huth, T.; Cryns, K.; Deforce, S.; Serneels, L.; Camacho, I. E.; Marjaux, E.; Craessaerts, K.; Roebroek, A. J. M.; Schwake, M.; D'Hooge, R.; Bach, P.; Kalinke, U.; Moechars, D.; Alzheimer, C.; Reiss, K.; Saftig, P.; De Strooper, B. *J. Biol. Chem.* **2005**, *280*, 30797.
30. Esterhazy, D.; Stuetzer, I.; Wang, H.; Rechsteiner, M. P.; Beauchamp, J.; Doebeli, H.; Hilpert, H.; Matile, H.; Prummer, M.; Schmidt, A.; Lieske, N.; Boehm, B.; Marselli, L.; Bosco, D.; Kerr-Conte, J.; Aebersold, R.; Spinas, G. A.; Moch, H.; Migliorini, C.; Stoffel, M. *Cell Metabolism* **2011**, *14*, 365.
31. Coordinates for the X-ray structure of compound **17h** complexed with BACE1 have been deposited in the Protein Data Bank (http://www.rcsb.org), and can be accessed under PDB ID 4DJX.
32. Korfmacher, W. A.; Cox, K. A.; Ng, K. J.; Veals, J.; Hsieh, Y.; Wainhaus, S.; Broske, L.; Prelusky, D.; Nomeir, A.; White, R. E. *Rapid Commun. Mass Spectrom.* **2001**, *15*, 335.
33. Coordinates for the X-ray structure of compound **24** complexed with BACE1 have been deposited in the Protein Data Bank (http://www.rcsb.org), and can be accessed under PDB ID 4DJY.